U.S. National Library of Medicine
National Center for Biotechnology Information

NLM Citation: Leung K. Cy5.5-Amino-terminal fragment of urokinase-type plasminogen activator conjugated to magnetic iron oxide nanoparticles. 2009 Oct 7 [Updated 2009 Dec 24]. In: Molecular Imaging and Contrast Agent Database (MICAD) [Internet]. Bethesda (MD): National Center for Biotechnology Information (US); 2004-2013.
Bookshelf URL: https://www.ncbi.nlm.nih.gov/books/

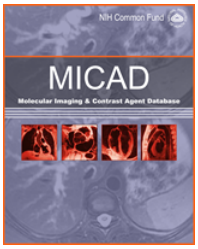

Cy5.5-Amino-terminal fragment of urokinase-type plasminogen activator conjugated to magnetic iron oxide nanoparticles

Cy5.5-AFT-IO

Kam Leung, PhD[1]

Created: October 7, 2009; Updated: December 24, 2009.

Chemical name:	Cy5.5-Amino-terminal fragment of urokinase-type plasminogen activator conjugated to magnetic iron oxide nanoparticles	
Abbreviated name:	Cy5.5-AFT-IO	
Synonym:		
Agent category:	Polypeptide	
Target:	Urokinase-type plasminogen activator receptor (uPAR)	
Target category:	Receptor	
Method of detection:	Magnetic resonance imaging (MRI), and optical, near-infrared (NIR) fluorescence imaging	
Source of signal:	Cy5.5, iron oxide	
Activation:	No	
Studies:	• *In vitro* • Rodents	Click on protein, nucleotide (RefSeq), and gene for more information about uPAR.

Background

[PubMed]

Magnetic resonance imaging (MRI) maps information about tissues spatially and functionally. Protons (hydrogen nuclei) are widely used in imaging because of their abundance in water molecules. Water comprises ~80% of most soft tissue. The contrast of proton MRI depends primarily on the density of the nucleus (proton spins), the relaxation times of the nuclear magnetization (T_1, longitudinal, and T_2, transverse), the magnetic environment of the tissues, and the blood flow to the tissues. However, insufficient contrast between normal and diseased tissues requires the development of contrast agents. Most contrast agents affect the T1 and T_2 relaxation times of the surrounding nuclei, mainly the protons of water. T_2^* is the spin–spin relaxation time composed of variations from molecular interactions and intrinsic magnetic heterogeneities of tissues in the magnetic field [1]. Cross-linked iron oxide (CLIO) nanoparticles and other iron oxide formulations affect T_2 primarily and lead to

Author Affiliation: 1 National Center for Biotechnology Information, NLM, NIH; Email: micad@ncbi.nlm.gov.

decreased signals. On the other hand, the paramagnetic T_1 agents, such as gadolinium (Gd^{3+}), and manganese (Mn^{2+}), accelerate T_1 relaxation and lead to brighter contrast images.

Optical fluorescence imaging is increasingly used to obtain biological functions of specific targets [2, 3] in small animals. However, the intrinsic fluorescence of biomolecules poses a problem when visible light (350-700 nm) absorbing fluorophores are used. Near-infrared (NIR) fluorescence (700-1000 nm) detection avoids the background fluorescence interference of natural biomolecules, providing a high contrast between target and background tissues. NIR fluorophores have wider dynamic range and minimal background as a result of reduced scattering compared with visible fluorescence detection. They also have high sensitivity, resulting from low infrared background, and high extinction coefficients, which provide high quantum yields. The NIR region is also compatible with solid-state optical components, such as diode lasers and silicon detectors. NIR fluorescence imaging is becoming a non-invasive alternative to radionuclide imaging in small animals.

Extracellular matrix (ECM) adhesion molecules consist of a complex network of fibronectins, collagens, chondroitins, laminins, glycoproteins, heparin sulfate, tenascins, and proteoglycans that surround connective tissue cells, and they are mainly secreted by fibroblasts, chondroblasts, and osteoblasts [4]. Cell substrate adhesion molecules are considered essential regulators of cell migration, differentiation, and tissue integrity and remodeling. These molecules play an important role in inflammation and atherogenesis, but they also participate in the process of invasion and metastasis of malignant cells in the host tissue [5]. Invasive tumor cells adhere to the ECM, which provides a matrix environment for permeation of tumor cells through the basal lamina and underlying interstitial stroma of the connective tissue. Overexpression of matrix metalloproteinases (MMPs) and other proteases by tumor cells allows intravasation of tumor cells into the circulatory system after degradation of the basement membrane and ECM [6]. Several families of proteases are involved in atherogenesis, myocardial infarction, angiogenesis, and tumor invasion and metastasis [7-10].

Urokinase-type plasminogen activator (uPA) is a serine protease [11, 12]. The uPA and uPA receptor (uPAR) system is responsible for tissue degradation after plasminogen activation to plasmin, which leads to a cascade of proteolysis or thrombolysis depending on the physiological conditions. uPA also directly activates MMPs, vascular endothelial growth factor, and human growth factor [13]. Malignant tumors and tumor-associated stromal cells (macrophages, endothelial cells and fibroblasts) often express high levels of uPA and uPAR [14]; therefore, the uPA/uPAR system is linked to vascular diseases and cancer. The amino-terminal fragment (ATF, 1-135 amino acids) of uPA binds with high affinity to uPAR [15]. Yang et al. [16] have developed a multimodality imaging probe by conjugation of Cy5.5-ATF to iron oxide nanoparticles to form Cy5.5-ATF-IO nanoparticles for NIR imaging and MRI of uPAR expression in tumor. Cy5.5 is a NIR fluorescent dye with absorbance maximum at 675 nm and emission maximum at 694 nm with a high extinction coefficient of 250,000 $M^{-1}cm^{-1}$.

Related Resource Links:

- Chapters in MICAD
- Gene information in NCBI (uPAR).
- Articles in OMIM
- Clinical trials (uPAR)
- Drug information in FDA

Synthesis

[PubMed]

Yang et al. [16] performed conjugation of Cy5.5 to recombinant ATF peptides with Cy5.5 maleimide. Paramagnetic iron oxide (IO) nanoparticles (10 nm core) coated with amphiphilic polymers were activated with

ethyl-3-dimethylaminopropyl-carbodiimide and sulfo-*N*-hydroxysuccinimide for 15 min. The activated nanoparticles were incubated with Cy5.5-ATF peptides (17 kDa) at a molar iron oxide to ATF of 1:20 at 4°C overnight. Cy5.5-ATF-IO nanoparticles (18 nm in diameter) were isolated with column chromatography. There were 8-10 Cy5.5-ATF peptides per nanoparticles.

In Vitro Studies: Testing in Cells and Tissues

[PubMed]

Kim et al. [15] performed binding experiments with ATF with the use of a Biacore sensor chip immobilized with uPAR. The K_d value of ATF was calculated to be 122 ± 13 nM. ATF inhibited endothelial cell proliferation induced with basic fibroblast growth factor (2 ng/ml) in culture with a 50% inhibition concentration of ~320 nM. The Kd for the Cy5.5-ATF-IO was not determined. Yang et al. [16] showed that Cy5.5-ATF-IO nanoparticles exhibited T_1-relaxivity R_1 values of 3.6 ± 0.3 mM^{-1} s^{-1} and T_2-relaxivity R_2 values of 124 ± 7 mM^{-1} s^{-1} at 3 T. Cy5.5-ATF-IO nanoparticles were internalized by mouse mammary carcinoma 4T1 cells (uPAR positive) but not by human mammary carcinoma T47D cells (uPAR negative). T_2-weighted imaging showed a signal reduction in 4T1 cells incubated with Cy5.5-ATF-IO nanoparticles compared with IO nanoparticles, whereas no signal reduction was observed in T47D cells.

Animal Studies

Rodents

[PubMed]

Yang et al. [16] performed T_2-weighted MR imaging (3 T) studies in mice bearing 4T1 tumors after intravenous injection of 0.2 nmol Cy5.5-ATF-IO nanoparticles. There was a 2-fold greater tumor signal reduction in the mice receiving Cy5.5-ATF-IO nanoparticles as compared with that in mice receiving IO nanoparticles at 6 h after injection. In contrast, the signal reduction was 50% and 80% less than that in mice receiving IO nanoparticles in the spleen and liver indicating non specific uptake of the IO nanoparticles. The signal reduction was similar in the kidney for both nanoparticles. Staining of iron in tissue sections confirmed the MRI findings. High resolution MR images showed the intracellular localization of nanoparticles in the cells. A high percentage of iron-positive cells were found in the tumor sections in mice injected with Cy5.5-ATF-IO nanoparticles but little or no iron-positive cells were detected in the tumor sections in mice injected with IO nanoparticles. Iron-positive cells were present in CD68-positive (macrophages) and CD68–negative cells (such as tumor cells). Optical imaging showed a strong Cy5.5 NIR fluorescence signal above the background was visualized in the tumor at 24 h after injection of Cy5.5-ATF-IO nanoparticles. The signal intensity increased at 48 h and decreased at 72 h as compared with the signal intensity at 24 h. The tumor/background ratios were 3.3, 2.2 and 2.0 at 24, 48 and 72 h, respectively. No blocking experiment was performed.

Other Non-Primate Mammals

[PubMed]

No publication is currently available.

Non-Human Primates

[PubMed]

No publication is currently available.

Human Studies

[PubMed]

No publication is currently available.

NIH Support

U54 CA119338, R01 CA133722, P50 CA128613

References

1. Wang Y.X., Hussain S.M., Krestin G.P. Superparamagnetic iron oxide contrast agents: physicochemical characteristics and applications in MR imaging. Eur Radiol. 2001;11(11):2319–31. PubMed PMID: 11702180.
2. Ntziachristos V., Bremer C., Weissleder R. Fluorescence imaging with near-infrared light: new technological advances that enable in vivo molecular imaging. Eur Radiol. 2003;13(1):195–208. PubMed PMID: 12541130.
3. Achilefu S. Lighting up tumors with receptor-specific optical molecular probes. Technol Cancer Res Treat. 2004;3(4):393–409. PubMed PMID: 15270591.
4. Bosman F.T., Stamenkovic I. Functional structure and composition of the extracellular matrix. J Pathol. 2003;200(4):423–8. PubMed PMID: 12845610.
5. Jiang W.G., Puntis M.C., Hallett M.B. Molecular and cellular basis of cancer invasion and metastasis: implications for treatment. Br J Surg. 1994;81(11):1576–90. PubMed PMID: 7827878.
6. Albelda S.M. Role of integrins and other cell adhesion molecules in tumor progression and metastasis. Lab Invest. 1993;68(1):4–17. PubMed PMID: 8423675.
7. Keppler D., et al. Tumor progression and angiogenesis: cathepsin B & Co. Biochem Cell Biol. 1996;74(6):799–810. PubMed PMID: 9164649.
8. Liu J., et al. Lysosomal cysteine proteases in atherosclerosis. Arterioscler Thromb Vasc Biol. 2004;24(8):1359–66. PubMed PMID: 15178558.
9. Berchem G., et al. Cathepsin-D affects multiple tumor progression steps in vivo: proliferation, angiogenesis and apoptosis. Oncogene. 2002;21(38):5951–5. PubMed PMID: 12185597.
10. Brix K., et al. Cysteine cathepsins: Cellular roadmap to different functions. Biochimie. 2007. PubMed PMID: 17825974.
11. Choong P.F., Nadesapillai A.P. Urokinase plasminogen activator system: a multifunctional role in tumor progression and metastasis. Clin Orthop Relat Res. 2003;(415 Suppl):S46–58. PubMed PMID: 14600592.
12. Rabbani S.A., Mazar A.P. The role of the plasminogen activation system in angiogenesis and metastasis. Surg Oncol Clin N Am. 2001;10(2):393–415. p. x. PubMed PMID: 11382594.
13. Folkman J., Shing Y. Angiogenesis. J Biol Chem. 1992;267(16):10931–4. PubMed PMID: 1375931.
14. Duffy M.J., et al. Urokinase plasminogen activator: a prognostic marker in multiple types of cancer. J Surg Oncol. 1999;71(2):130–5. PubMed PMID: 10389872.
15. Kim K.S., et al. Differential inhibition of endothelial cell proliferation and migration by urokinase subdomains: amino-terminal fragment and kringle domain. Exp Mol Med. 2003;35(6):578–85. PubMed PMID: 14749538.
16. Yang L., et al. Receptor-targeted nanoparticles for in vivo imaging of breast cancer. Clin Cancer Res. 2009;15(14):4722–32. PubMed PMID: 19584158.